



**HAL**  
open science

## Identification of a Grotthuss Proton Hopping Mechanism at Protonated Polyhedral Oligomeric Silsesquioxane (POSS) -Water Interface

K. R. Maiyelvaganan, S Kamalakannan, S. Shanmugan, M. Prakash,  
François-Xavier Coudert, M. Hochlaf

► **To cite this version:**

K. R. Maiyelvaganan, S Kamalakannan, S. Shanmugan, M. Prakash, François-Xavier Coudert, et al.. Identification of a Grotthuss Proton Hopping Mechanism at Protonated Polyhedral Oligomeric Silsesquioxane (POSS) -Water Interface. *Journal of Colloid and Interface Science*, 2022, 605, pp.701-709. 10.1016/j.jcis.2021.07.115 . hal-03312838

**HAL Id: hal-03312838**

**<https://hal.science/hal-03312838>**

Submitted on 2 Aug 2021

**HAL** is a multi-disciplinary open access archive for the deposit and dissemination of scientific research documents, whether they are published or not. The documents may come from teaching and research institutions in France or abroad, or from public or private research centers.

L'archive ouverte pluridisciplinaire **HAL**, est destinée au dépôt et à la diffusion de documents scientifiques de niveau recherche, publiés ou non, émanant des établissements d'enseignement et de recherche français ou étrangers, des laboratoires publics ou privés.

# Identification of a *Grotthuss* Proton Hopping Mechanism at Protonated Polyhedral Oligomeric Silsesquioxane (POSS) – Water Interface

**K. R. Maiyelvaganan,<sup>§</sup> S. Kamalakannan,<sup>§</sup> S. Shanmugan,<sup>§</sup> M. Prakash,<sup>§,\*</sup> F.-X. Coudert,<sup>‡,\*</sup> and M. Hochlaf<sup>§,\*</sup>**

<sup>§</sup> Department of Chemistry, Faculty of Engineering and Technology, SRM Institute of Science and Technology, SRM Nagar, Kattankulathur-603203, Chennai TN, India.

<sup>‡</sup> Chimie ParisTech, PSL University, CNRS, Institut de Recherche de Chimie Paris, 75005 Paris, France.

<sup>§</sup> Université Gustave Eiffel, COSYS/LISIS, 5 Bd Descartes 77454, Champs sur Marne, France.

---

\* Authors for correspondence:

M.P.: Phone: +91 2741 7686. Email: [prakashspm@gmail.com](mailto:prakashspm@gmail.com) and [prakashm4@srmist.edu.in](mailto:prakashm4@srmist.edu.in) ORCID: 0000-0002-1886-7708

F.-X.C.: Email: [fx.coudert@chimieparistech.psl.eu](mailto:fx.coudert@chimieparistech.psl.eu) ORCID: 0000-0001-5318-3910

M.H: Email: [hochlaf@univ-mlv.fr](mailto:hochlaf@univ-mlv.fr) ORCID: 0000-0002-4737-7978

## Abstract

The attachment and dissociation of a proton from a water molecule and the proton transfers at solid-liquid interfaces play vital roles in numerous biological, chemical processes and for the development of sustainable functional materials for energy harvesting and conversion applications. Using first-principles computational methodologies, we investigated the protonated forms of polyhedral oligomeric silsesquioxane (POSS-H<sup>+</sup>) interacting with water clusters (W<sub>n</sub>, where  $n = 1-6$ ) as a model to quantify the proton conducting and localization ability at solid-liquid interfaces. Successive addition of explicit water molecules to POSS-H<sup>+</sup> shows that the assistance of at least three water molecules is required to dissociate the proton from POSS with the formation of an Eigen cation (H<sub>9</sub>O<sub>4</sub><sup>+</sup>), whereas the presence of a fourth water molecule highly favors the formation of a Zundel ion (H<sub>5</sub>O<sub>2</sub><sup>+</sup>). Reaction pathway and energy barrier analysis reveal that the formation of the Eigen cation requires significantly higher energy than the Zundel features. This confirms that the Zundel ion is destabilized and promptly converts in to Eigen ion at this interface. Moreover, we identified a Grotthuss-type mechanism for the proton transfer through a water chain close to the interface, where symmetrical and unsymmetrical arrangements of water molecules around H<sup>+</sup> of protonated POSS-H<sup>+</sup> are involved in the conduction of proton through water wires where successive Eigen-to-Zundel and Zundel-to-Eigen transformations are observed in quick succession.

**Keywords:** DFT, AIM, AIMD, Grotthuss, POSS, Protonated Water Clusters, IR Signatures, Eigen and Zundel

## 1. Introduction

Proton transport and conduction of proton through water chains occur in a variety of atmospheric, biological and chemical processes.<sup>1,2,3,4,5,6,7</sup> The formation of hydronium ion and the mobility of the proton is on the origins of these phenomena. For explanation, two scenarios were suggested: (i) Back in 1806, von Grotthuss<sup>8</sup> proposed a mechanism, which makes it possible to account for the high ionic molar conductivity of hydronium and hydroxide ions and thus of water liquid conductivity. Within this mechanism, the ion does not have to move entirely through the liquid to carry its charge, but only passes the excess proton. Indeed, each oxygen atom passes and at the same time receives a hydrogen atom. Obviously, Grotthuss-type of proton transfer is rapid and efficient, where water facilitates an efficient charge separation when the proton leaves the acid. If it occurs at the interfaces of liquid water with biological entities, or catalysts or material interfaces, it changes drastically the kinetics and thus the outcomes and applications of such compounds. (ii) Alternatively, Kreuer, Rabenau, and Weppner<sup>9</sup> established in 1982 a mechanism (denoted as “vehicle mechanism”) where the protons attached to the protonated species and the neutral surrounding uncharged molecules diffuse together. The excess proton travels on top of the host molecule through the solvent. The vehicle mechanism corresponds hence mostly to the proton conduction in aqueous systems.

The solid-liquid interface proton transfers are important for fuel cell applications such as the proton conduction in electrolyte membranes. The commonly used Nafion-based membranes have however some drawbacks limiting their applications.<sup>10</sup> Exploiting alternative composite fuel cell membranes without compromising proton conductivity is an active field. For that purposes, polyhedral oligosilsesquioxanes (POSS) as nano-additives are expected to enhance the properties of such cells. This is also associated with good thermal, chemical and mechanical stabilities because of the rigidity of the inner silicon and oxygen frameworks.<sup>11,12</sup> Indeed, earlier experimental studies highlighted the benefits of POSS framework such as its non-volatility and its extensively stable nature at high temperature, pressure, odorless, extreme acid-base condition. It is also ecologically friendly.<sup>13,14,15</sup>

It is very challenging to probe the mobility of protons at the solid-liquid interface using experimental techniques. Instead, insights into the proton transfer mechanism, pathway and conduction ability of materials can be understood by a variety of computational and dynamical techniques.<sup>16,17,18,19,20,21,22</sup> For instance, the proton transfer in aqueous media and proton dissociation ability from acidic materials have been studied using the density functional theory (DFT) and *ab initio* electronic structure approaches.<sup>23,24</sup> There are however few studies that have been reported on POSS-based materials for proton conduction ability of sulfonic acid or phosphonic acid derivatives.<sup>25,26</sup>

At present, quantum chemical calculations using *ab initio* and DFT methods are performed for understanding the acidic nature of POSS-H<sup>+</sup> cage as well as the proton transfer, the proton conduction

pathway and proton affinity in this solid-liquid interface. This is done after structural changes and symmetric, asymmetric, proton oscillation and strong hydrogen bond (H-bond) stretch vibrational analyses of the protonated form of polyhedral oligomeric silsesquioxane with water (W) clusters (POSS-H<sup>+</sup>@W<sub>n</sub>, where  $n = 1 - 6$ ). In addition, we show that the protonated species participate into a proton hopping mechanism at this solid-liquid interface *via* Grotthuss-type mechanism. The excess proton dissociation from POSS-H<sup>+</sup> molecule to water molecule is associated with the successive formation of Eigen/Zundel/Eigen cations. Their vital role in proton transfer process at microscopic level is elucidated. This process was already observed at silica–water interface,<sup>22</sup> but it is found here for the first time for an interface composed by a nano-cluster and water molecules.

## 2. Methodologies

### 2.1 Characterization of POSS-H<sup>+</sup>@W<sub>n</sub> ( $n = 1 - 6$ ) clusters

The initial structure of POSS was taken from crystal database of POSS framework. For the initial structure of POSS-H<sup>+</sup>, we used the procedure described in Figure S1. All geometry optimizations were done at the DFT level, using the B3LYP functional (Becke’s three-parameter hybrid exchange functional and Lee-Yang-Parr correlation functional), in conjunction with the 6-311++G\*\* basis set.<sup>27,28</sup> Earlier reports revealed that this level of basis set is suitable to study accurately the structure, stability and spectral signatures of protonated water clusters and proton transfer mechanism.<sup>29,30,31,32</sup> Geometry optimizations were systematically followed by frequency calculations carried out at the same level of theory, to confirm the minimal nature of the stationary points on the corresponding potential energy surface. All electronic structure calculations were performed using *GAUSSIAN 16*.<sup>33</sup> *GaussView 6.0* and *Chemcraft* softwares were used for visualization and geometrical analysis.<sup>34,35</sup> We also performed atoms in molecules (AIM) analysis using the AIM2000 package<sup>36</sup> to quantify the various types of noncovalent interactions in POSS-H<sup>+</sup>@Water interfaces (see Supporting Information for full details).

### 2.2 *Ab initio* molecular dynamics (AIMD) methodology

The hybrid Gaussian and plane wave method GPW was used as implemented in the CP2K software.<sup>37</sup> The production simulations were performed in the constant-volume ( $N, V, T$ ) ensemble with fixed size and shape of the unit cell. A time step of 0.5 fs was used in the MD runs, and the temperature was controlled by using a canonical sampling through velocity rescaling thermostat with a time constant of 1 ps. The exchange-correlation energy was evaluated in the Perdew–Burke–Ernzerhof (PBE) approximation<sup>38</sup> and the dispersion interactions were treated by incorporating Grimme corrections<sup>39,40</sup> at the DFT-D3 level. The Quickstep module uses a multigrid system to map the basis functions onto. The default number of 4 different grids was used, along with a plane-wave cutoff for the electronic density of 800 Ry (suited for the presence of O atoms), and a relative cutoff of 40 Ry. Valence electrons were

described by double- $\zeta$  valence polarized basis sets and norm-conserving Goedecker–Teter–Hutter pseudopotentials all adapted for PBE (DZVP-GTH-PBE) for H, C, O and Si. In addition, to identify the proton transfer reaction pathways and to get more insights on the ionic features of protonated water clusters at this interface, we have performed Nudged elastic band (NEB) calculations with PBE+D3 method, where the atoms were described with the triple- $\zeta$  valence polarized basis sets (TZVP-GTH-PBE) for H, O and Si atoms.

The present methodology relies on the GGA-level exchange–correlation functional PBE, with dispersion corrections, to describe the water and water–POSS interactions. While this level of theory is known to slightly over structure water systems (including the liquid phase), this is in balance with a lower computational cost that allows for better statistical sampling. Given the system sizes and MD length involved in this study, hybrid functionals could not be used. Furthermore, we note that GGA-level exchange–correlation functionals are widely used for the description of water near interfaces, including in the description of Grothuss proton transfer, and are qualitatively well validated. This includes a wide range of systems and phenomena, such as chemically reactive graphene oxide in water<sup>41</sup>, inorganic or mineral surface/water interface<sup>42,43</sup>, boron nitride and graphene<sup>44</sup>, etc. ...

### **3. Results**

#### **3.1 Structures of POSS-H<sup>+</sup>@W<sub>n</sub> (n = 1 – 6) clusters**

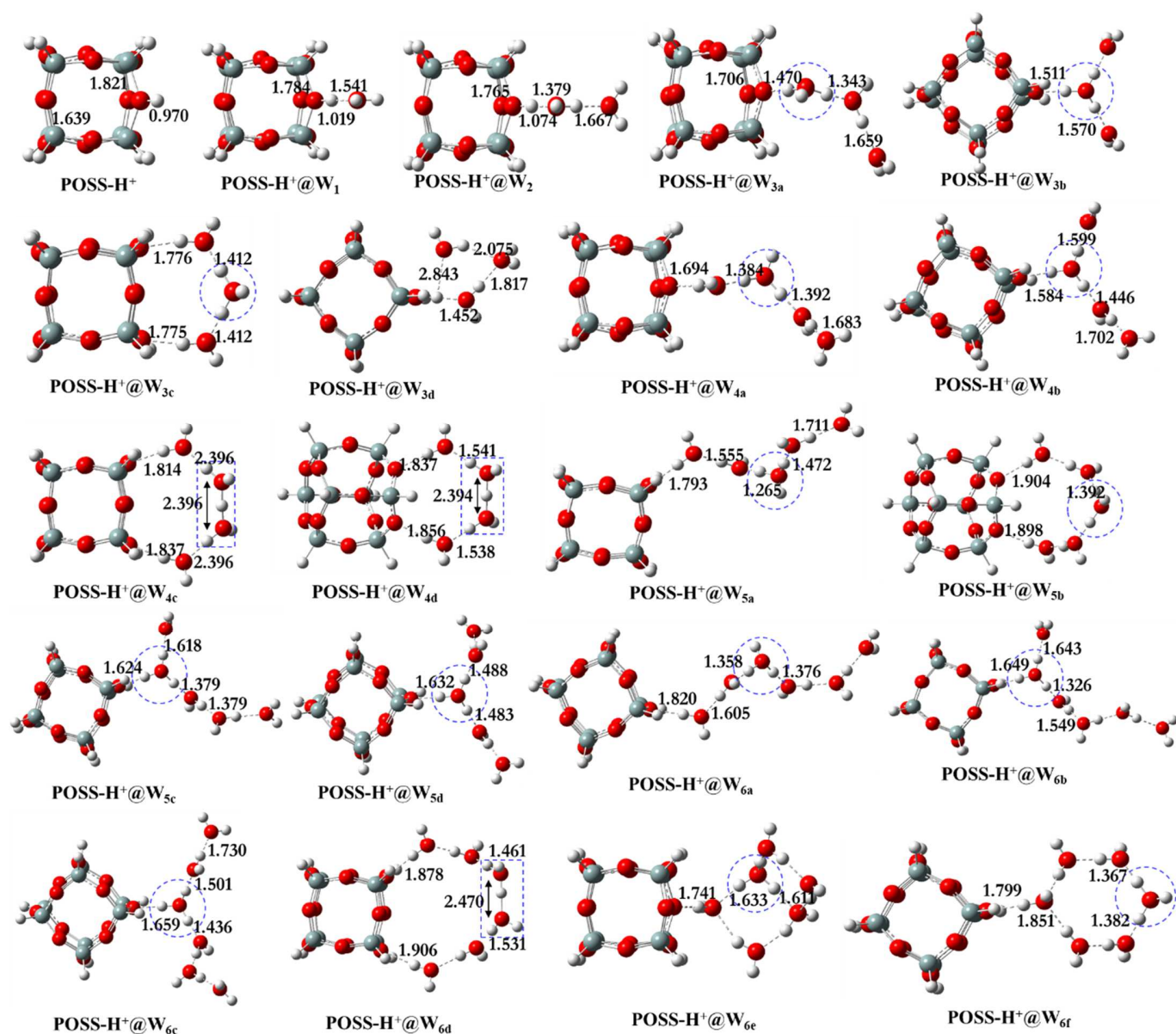


**Figure 1:** B3LYP/6-311++G\*\* optimized geometries of protonated polyhedral oligomeric silsesquioxane water clusters (POSS-H<sup>+</sup>@W<sub>n</sub>; where  $n = 1 - 6$ ). Distances are in Å. The dashed blue circle and rectangle highlights the formation of H<sub>3</sub>O<sup>+</sup> and H<sub>5</sub>O<sub>2</sub><sup>+</sup> cations, respectively.

Figure 1 displays the optimized geometries of POSS-H<sup>+</sup>@W<sub>n</sub> ( $n=1-6$ ) clusters. This figure gives also the main distances between POSS-H<sup>+</sup> and water molecules. For POSS-H<sup>+</sup> and POSS-H<sup>+</sup>@W<sub>1</sub> and POSS-H<sup>+</sup>@W<sub>2</sub> a unique form is found. For POSS-H<sup>+</sup>@W<sub>3</sub>, POSS-H<sup>+</sup>@W<sub>4</sub> and POSS-H<sup>+</sup>@W<sub>5</sub>, four stable configurations are identified. For POSS-H<sup>+</sup>@W<sub>6</sub>, we obtain six stable structures. Within all species, the POSS moiety adopts a similar cube-like geometry, which is analogous to the cubane framework: Si atoms

are placed at the corners of the cube and bridging oxygen atoms are in-between two Si atoms. For the optimized structure of POSS, the angles are  $149^\circ$  and  $109^\circ$  for the Si-O-Si and O-Si-O linkages, respectively (Figure S1). These parameters are in very close agreement with the experimental crystal structure of POSS.<sup>45</sup> Upon protonation, the additional proton links to an oxygen atom and the corresponding O-H bond distance is  $0.970 \text{ \AA}$ . The corners of the cuboid structure in the vicinity of this protonated oxygen are affected by the presence of the  $\text{H}^+$ , and we compute Si-O-Si  $\sim 132^\circ$  and O-Si-O  $\sim 105^\circ$ .

Upon addition of water molecules to  $\text{POSS-H}^+$ , we found that the proton strongly interacts with the primary shell formed by water. Depending on the geometry and number of water molecules, we observe either the lengthening of the distance between the proton and the oxygen of POSS, or the proton transfer from  $\text{POSS-H}^+$  to the water cluster. For instance, this distance increases from  $0.970 \text{ \AA}$  in  $\text{POSS-H}^+$  to  $1.019 \text{ \AA}$  in  $\text{POSS-H}^+@W_1$  and to  $1.074 \text{ \AA}$  in  $\text{POSS-H}^+@W_2$ . At the same time, the  $\text{H}^+\cdots\text{O}_w$  distance ( $\text{O}_w$  is the O of the water molecule) decreases and the H-bond becomes shorter and stronger. Additional water molecules attached to  $\text{POSS-H}^+@W_2$  lead to proton dissociation from  $\text{POSS-H}^+$  and attachment to the neighboring water molecule. This is associated with the formation of either an Eigen cation core or a Zundel cation core at the water chain. The latter requires minimum of four water molecules interacting with  $\text{POSS-H}^+$ . This is the case for all  $\text{POSS-H}^+@W_n$  (where,  $n = 3-6$ ) structures except the one denoted as  $\text{POSS-H}^+@W_{3d}$  (Figure 1). These cations are stabilized by linear, branched or cyclic H-bond patterns. Specifically, we notice an excess proton on water clusters. When possible, we assist to the complete solvation of the Eigen cation to further stabilize this ion. For the Zundel ion, the excess proton is localized in the middle of the two water molecules with the formation of Zundel core (highlighted by the blue dashed rectangle in Figure 1) and the proton donor and acceptor sites in the rigid POSS materials. This is associated with a planar water six-membered ring. The excess proton is dangling between two water molecules ( $\text{H}_2\text{O}\cdots\text{H}^+\cdots\text{O}_w$ ) with a distance of  $2.4 \text{ \AA}$ , which is typical for Zundel ion.<sup>46</sup>

### 3.2 Binding energies

To get insights on the stability and the mechanism of the proton transfer on the  $\text{POSS-H}^+@W_n$  ( $n = 1-6$ ) clusters, we computed their binding energies (BE). The BEs were calculated using the supermolecular approach and corrected for basis set superposition error (BSSE) employing the counterpoise (CP) procedure suggested by Boys and Bernardi<sup>47</sup>

$$BE = \left( E_{Cluster} - \sum_{i=1}^n E_i \right) \quad (1)$$

where,  $E_{Cluster}$  is the total energy of the  $\text{POSS-H}^+@W_n$  cluster,  $E_i$  is the energy of the monomers (i.e. POSS,  $\text{POSS-H}^+$ ,  $\text{H}_2\text{O}$  or  $\text{H}_3\text{O}^+/\text{H}_2\text{O}_5^+$ ). To quantify the dispersion energy in these clusters, we have computed energetics both with (DFT-D3) and without (DFT) the inclusion of Grimme's dispersion correction on the

DFT optimized structures.<sup>48</sup> The BSSE-corrected BEs of various POSS-H<sup>+</sup>@W<sub>n</sub> (n = 1-6) clusters are given in Table 1. As can be seen there, the BEs including the D3 corrections are larger (in absolute value), and they will be considered for the discussion as being in principle more accurate. For POSS-H<sup>+</sup>@W<sub>n</sub> (n ≥ 3) clusters, the Eigen core cyclic clusters are more stable than the other isomers.

**Table 1:** BSSE corrected binding energies (BE in kcal/mol) with and without considering the dispersion correction (+D3) for the POSS-H<sup>+</sup>@W<sub>n</sub> (where n=1-6) clusters using the B3LYP/6-311++G\*\* method. N<sub>HB</sub> corresponds to the number of Hydrogen bonds.

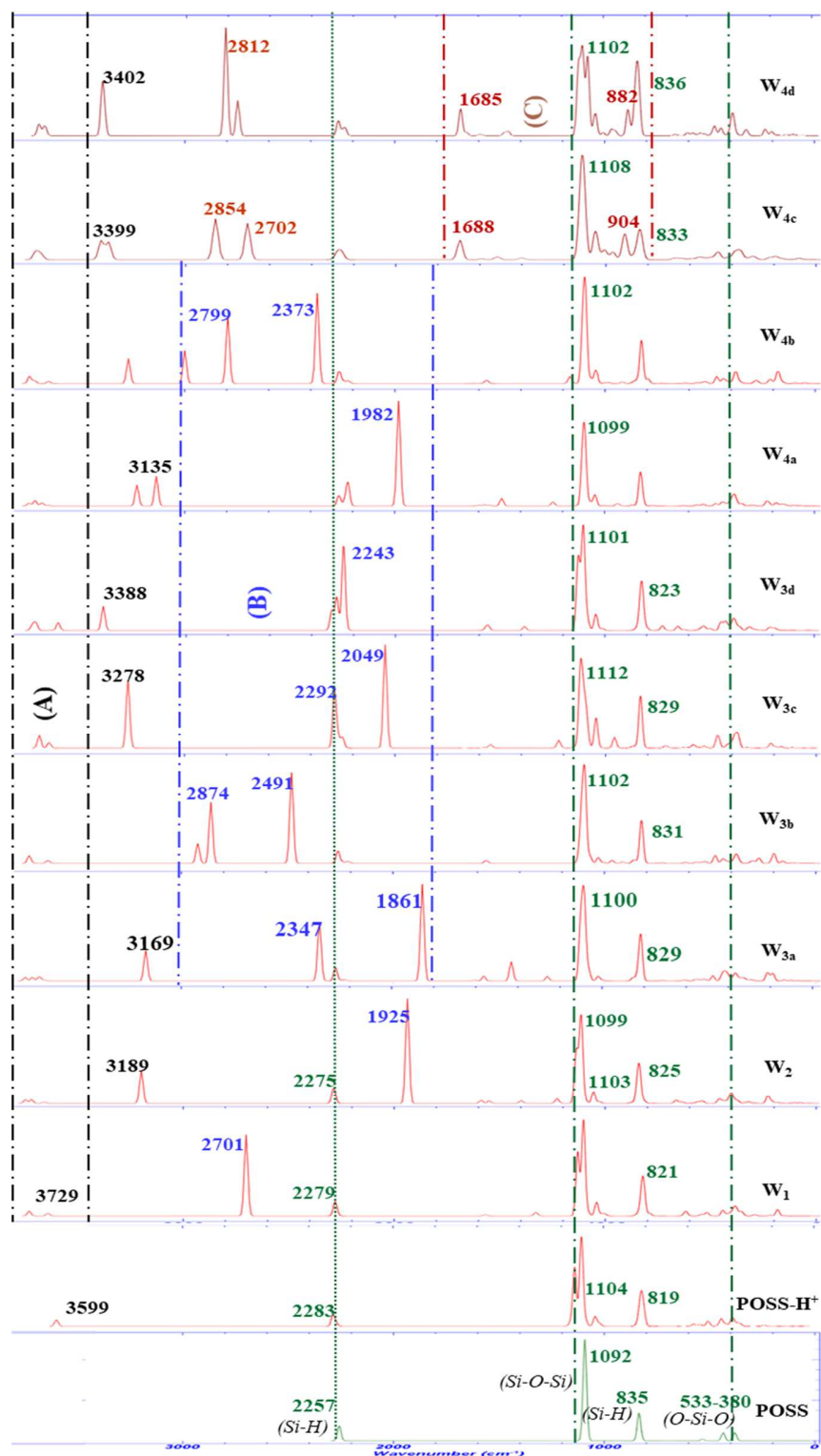
| POSS-H <sup>+</sup> @W <sub>n</sub>  | Ionic defect in water clusters          | BE     |         | N <sub>HB</sub> | BE/N <sub>HB</sub> |
|--------------------------------------|---|--------|---------|-----------------|--------------------|
|                                      |   | BSSE   | BSSE+D3 |                 | BSSE+D3            |
| POSS-H <sup>+</sup> @W <sub>1</sub>  | H-Bond with W <sub>1</sub>              | -21.4  | -23.1   | 1               | -23.1              |
| POSS-H <sup>+</sup> @W <sub>2</sub>  | H-Bond in W <sub>2</sub> chain          | -40.8  | -43.7   | 2               | -21.8              |
| POSS-H <sup>+</sup> @W <sub>3a</sub> | Eigen in W <sub>3</sub> chain           | -84.7  | -89.1   | 3               | -29.7              |
| POSS-H <sup>+</sup> @W <sub>3b</sub> | Eigen in POSS-W interface               | -81.9  | -86.6   | 3               | -28.9              |
| POSS-H <sup>+</sup> @W <sub>3c</sub> | Eigen in cyclic W <sub>3</sub>          | -86.0  | -93.0   | 4               | -23.3              |
| POSS-H <sup>+</sup> @W <sub>3d</sub> | H-Bonded W <sub>n</sub> Cluster         | -44.8  | -51.3   | 3               | -17.1              |
| POSS-H <sup>+</sup> @W <sub>4a</sub> | Eigen in W <sub>4</sub> chain           | -95.3  | -100.2  | 4               | -25.1              |
| POSS-H <sup>+</sup> @W <sub>4b</sub> | Eigen in POSS-W interface               | -94.7  | -100.3  | 4               | -25.1              |
| POSS-H <sup>+</sup> @W <sub>4c</sub> | Formation of Zundel                     | -58.7  | -65.3   | 4               | -16.3              |
| POSS-H <sup>+</sup> @W <sub>4d</sub> | Formation of Zundel                     | -58.0  | -64.5   | 4               | -16.1              |
| POSS-H <sup>+</sup> @W <sub>5a</sub> | Eigen in W <sub>5</sub> chain           | -111.6 | -117.3  | 5               | -23.5              |
| POSS-H <sup>+</sup> @W <sub>5b</sub> | Eigen cyclic W <sub>5</sub>             | -109.7 | -117.8  | 6               | -19.6              |
| POSS-H <sup>+</sup> @W <sub>5c</sub> | Eigen in POSS-W interface               | -107.2 | -119.2  | 5               | -23.8              |
| POSS-H <sup>+</sup> @W <sub>5d</sub> |   | -106.5 | -112.9  | 5               | -22.6              |
| POSS-H <sup>+</sup> @W <sub>6a</sub> | Eigen in W <sub>6</sub> chain           | -119.1 | -125.5  | 6               | -20.9              |
| POSS-H <sup>+</sup> @W <sub>6b</sub> | Eigen in POSS-W interface               | -119.2 | 126.3   | 6               | -21.1              |
| POSS-H <sup>+</sup> @W <sub>6c</sub> |   | -117.5 | -124.8  | 6               | -20.8              |
| POSS-H <sup>+</sup> @W <sub>6d</sub> | Zundel formation in W <sub>6</sub> Ring | -81.3  | -84.0   | 6               | -14.0              |
| POSS-H <sup>+</sup> @W <sub>6e</sub> | Eigen in W <sub>6</sub> Book            | -119.0 | -129.3  | 8               | -16.2              |
| POSS-H <sup>+</sup> @W <sub>6f</sub> | Eigen in W <sub>6</sub> Ring            | -120.8 | -129.1  | 7               | -18.4              |

Table 1 shows that the |BE|'s increase from 20 to 120 kcal/mol when increasing the number of water molecules. This is due to the improved stabilization of the larger complexes by H-bonds, yet typical

H-bond energies are in the range of  $\sim 5\text{--}10$  kcal/mol, i.e., much less than the bond energies of our interface material. The existence of Eigen core with water clusters is significantly more stable than the non-Eigen containing complexes (e.g. POSS-H<sup>+</sup>@W<sub>3d</sub>; Figure 1 and Table 1). Also, the Eigen core clusters are more stable than the corresponding Zundel type having the same H-bonds; this is due to the positive charge delocalization (i.e. equally shared) between two water molecules. Thus, the existence of Eigen core with water clusters significantly stabilizes this solid@water interface model. In contrast, the formation of Zundel cation relatively destabilizes this interface. Table 1 shows indeed that there is a reduction of |BE| for the corresponding clusters. For illustration, Table 1 gives the BE/N<sub>HB</sub> quantity which corresponds to the BE per H-bond within the complex. They are in the range -15 to -30 kcal/mol with minimal values for clusters having Zundel ion structure or H-bonded W<sub>n</sub> cluster. We further note that both clusters having Zundel motifs possess BE/N<sub>HB</sub> of  $\sim -16.0$  kcal/mol which is close to the value for the Zundel ion (H<sup>+</sup>(H<sub>2</sub>O)<sub>2</sub>) optimized at the MP2 level of theory.<sup>49</sup>

### 3.3 IR spectra

For better highlighting the effects of clustering of POSS-H<sup>+</sup> and to help their identification in the laboratory, we generated the IR spectra of POSS-H<sup>+</sup>@W<sub>n</sub>. The vibrational frequencies are reported after scaling the harmonic frequencies by a factor of 0.9577, for ease of comparison with experimental data.<sup>50</sup> The full analysis of the data is given in the Supporting Information (Table S2). For illustration, Figure 2 presents the simulated spectrum of POSS-H<sup>+</sup>@W<sub>n</sub> ( $n = 1\text{--}4$ ) clusters. The calculated characteristic intense peaks of POSS framework materials for Si-O-Si bending and Si-H stretching are observed at  $\sim 1104$ ,  $2260$  cm<sup>-1</sup>, respectively in good agreement with the corresponding experimental stretching frequencies ( $1100$  cm<sup>-1</sup> and  $2293$  cm<sup>-1</sup>).<sup>45</sup> Similarly, the calculated IR spectrum of O-Si-O linkage of  $\nu_{as}$  ( $380$  cm<sup>-1</sup>),  $\nu_{ss}$  ( $533$  cm<sup>-1</sup>) and Si-H oscillations peak ( $862$  cm<sup>-1</sup>) values are also in very good agreement with experimental values which are  $389$ ,  $557$  and  $860$  cm<sup>-1</sup>, respectively. This confirms the good accuracy of the present predictions. Note that the vibrational results analyses are in good agreement with the geometrical parameters and AIM electron density topography analyses. (See Supporting Information for details).



**Figure 2:** B3LYP/6-311++G\*\* calculated gas phase IR spectrum of the POSS-H<sup>+</sup>@W<sub>n</sub> (n=1-4) clusters. The three component bands (A) (black), (B) (blue) and (C) (brown) correspond to free water O-H stretching, to Eigen core to water stretching and to Zundel core proton oscillation, respectively.

The calculated IR spectra of POSS-H<sup>+</sup>@W<sub>n</sub> (*n* = 1–4) clusters are shown in Figure 2. For POSS-H<sup>+</sup>@W<sub>1</sub>, the peaks appear at 3640 and 3729 cm<sup>-1</sup> due to the symmetric and asymmetric O-H stretching of water molecule in two free O-H groups. Compared to a free water molecule, these values are slightly red shifted by ~ 16 and 28 cm<sup>-1</sup> respectively. The intense band at 2701 cm<sup>-1</sup> corresponds to the H-bonded acceptor water (A) molecule with the POSS-H<sup>+</sup> moiety. The corresponding red shifted value is 897 cm<sup>-1</sup>. Such large redshift is a signature of the strength of the H-bonds in these clusters. In POSS-H<sup>+</sup>@W<sub>2</sub> cluster, the H-bonded AD water molecule gives intense band at 1925 cm<sup>-1</sup> and resulting in a red shift of 1674 cm<sup>-1</sup>. The large red shift is due to the presence of charge movement towards H-bonded water chain and the subsequent O-H bond order decrease. Earlier reports revealed that the calculated red shift value of acceptor (A) is significantly higher than the less acceptor (A) or donor (D) types of H-bond.<sup>3,17,54</sup> For POSS-H<sup>+</sup>@W<sub>3</sub> clusters, there is an Eigen core stretching band around 2347 cm<sup>-1</sup>, which is slightly red shifted with real Eigen core in aqueous medium (i.e. 2420 cm<sup>-1</sup>). Both AD and A types H-bond stretching frequencies are observed for water trimer.

The IR spectra of POSS-H<sup>+</sup>@W<sub>4</sub> isomers exhibit both Eigen and Zundel features. The bands at 1982 and 2373 cm<sup>-1</sup> for POSS-H<sup>+</sup>@W<sub>4a</sub> and POSS-H<sup>+</sup>@W<sub>4b</sub> clusters are due to Eigen core stretching A and AD water molecules. The larger red shift corresponds to linear type clusters, which is more favorable for the proton transport through water chain. The excess proton always stabilizes in the middle of the water chain, irrespective the *n* value. Also, we observe Zundel features in POSS-H<sup>+</sup>@W<sub>4c</sub> and POSS-H<sup>+</sup>@W<sub>4d</sub> clusters. The respective O-H<sup>+</sup>-O oscillation vibrational modes appear at 1688 and 1685 cm<sup>-1</sup>. In addition, low frequency modes are computed at 904 and 882 cm<sup>-1</sup> for the Zundel characteristic peaks. Since the linear chain Eigen water interactions are stronger than the cyclic and branched water clusters, a large red shift is computed.

### 3.4 Dynamics of proton transfer at the POSS-Water interface

To probe the dynamics of the POSS-H<sup>+</sup>@water proton transfer, we then performed *ab initio* molecular dynamics (AIMD) simulations, also known as first-principles MD. The protocol followed was the following: (i) generate an initial configuration by random packing the POSS-H<sup>+</sup> with 53 water molecules in a 12 Å cubic box; (ii) perform a short geometry optimization of the water molecules, to relax possible unphysical configurations due to random packing; (iii) run a constant-pressure dynamics (NPT MD) with the POSS-H<sup>+</sup> frozen, so that the density can relax to its equilibrium value, and the water can reorient and solvate the POSS-H<sup>+</sup>; (iv) run a “production” constant-temperature dynamics (NVT MD) at the average volume, allowing all atoms to move freely. This computational protocol ensures that the POSS-H<sup>+</sup>@water dynamics start from a physically meaningful configuration, and we can focus observation on the dynamics

of the proton. We studied the system at two temperatures, 100 K and 300 K, and performed 3 simulations at each temperature.

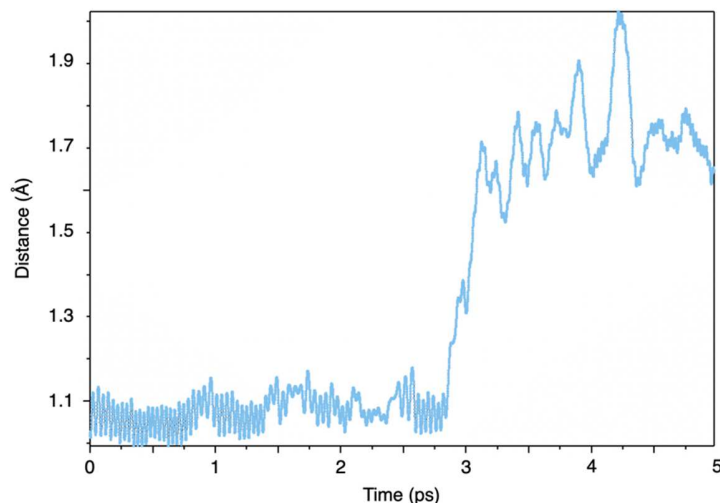


**Figure 3:**  $\text{O}^*-\text{H}^+$  distance as a function of time during a 100 K AIMD simulation, where  $\text{O}^*$  is the oxygen atom of the POSS originally bonded to the excess proton in  $\text{POSS}-\text{H}^+$ .

In the majority of cases, we observe a spontaneous transfer for  $\text{H}^+$  from  $\text{POSS}-\text{H}^+$  to the water. This is clearly manifested in the plot of  $\text{O}^*-\text{H}^+$  distance over time (Figure 3), if we label  $\text{O}^*$  the POSS oxygen that initially bears the proton: in this 100 K dynamics, we see that the initial structure (solvated  $\text{POSS}-\text{H}^+$ ) is stable in water for the first 2.8 ps of the trajectory, after which we observe a proton transfer to form  $\text{POSS} + \text{H}_3\text{O}^+$ . We also see that the hydronium cation remains weakly hydrogen-bonded to the neutral POSS, even in solution, as the  $\text{O}^*-\text{H}^+$  distance fluctuates around 1.75 Å (characteristic of a H bond). Further simulation shows that the excess proton can then diffuse by a Grotthuss-like mechanism, which AIMD is known to be well-suited to reproduce, both in bulk<sup>51</sup> and at interfaces<sup>52</sup>. We have observed several events of proton transfer between water molecules (4 times during the dynamics at 300 K), and the simulation was not continued after that: as the excess proton goes further away from the POSS, its dynamics will be that of the excess proton in liquid water.

In some cases, we have also observed reactive events involving the POSS itself, i.e. strong deformation leading to bond breaking inside the Si—O framework, in a relatively short time (100 to 300 fs). This was observed in one case at each temperature, and while the details of the dynamics leading to this chemical event vary, the event itself is the same in both cases: if we name  $\text{O}^*$  the POSS oxygen that initially bears the proton, then one of the Si— $\text{O}^*$  bonds breaks (see Figure 4). On one side it forms  $-\text{Si}-\text{OH}$ , which reorients to some extent but does not react further. On the other side, the now-undercoordinated Si will

bond to one of the water molecules, forming  $-\text{Si}-\text{OH}_2^+$ ; this will then very rapidly transfer its excess proton to a neighboring water molecule, ultimately leading to the formation of  $-\text{Si}-\text{OH}$  and  $\text{H}_3\text{O}^+$  (as depicted on Figure 4). The excess proton then diffuses by a Grotthuss-like mechanism.

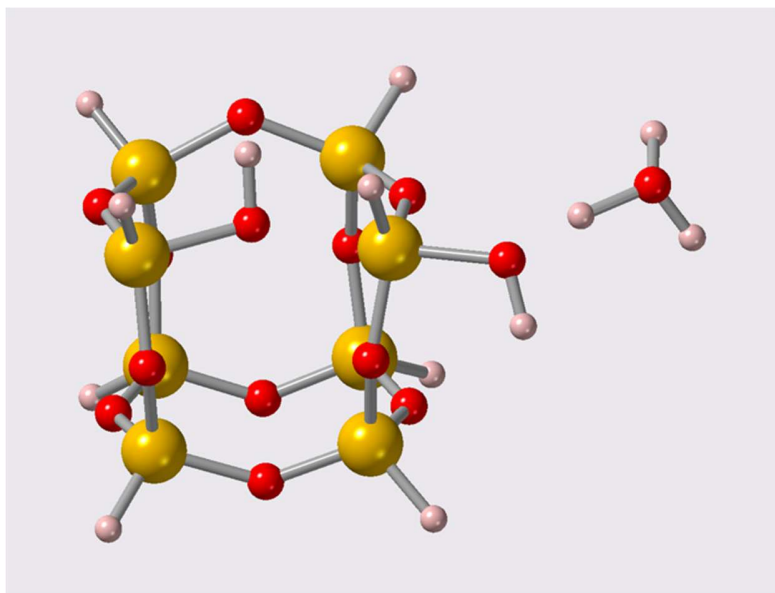


**Figure 4:** Final structure after reactivity of the POSS- $\text{H}^+$  system with water, as observed in AIMD (see text for details); 52 water molecules not directly involved in the chemical event are not displayed, for the sake of clarity.

Therefore, the AIMD study confirms the conclusions of a Grotthuss-type mechanism for transfer of proton in this POSS- $\text{H}^+$ @water system. It also suggests that, in liquid water (or in presence of more than a few water molecules), there are other possible evolutions of the POSS- $\text{H}^+$  system, including reactivity of the POSS framework itself. This will need to be further investigated by systematic exploration of the potential energy surface of the POSS- $\text{H}^+$ @ $\text{W}_n$  configurations taking into account such opening, or by more computational expensive free energy methods based on the AIMD description.

#### 4. Discussion

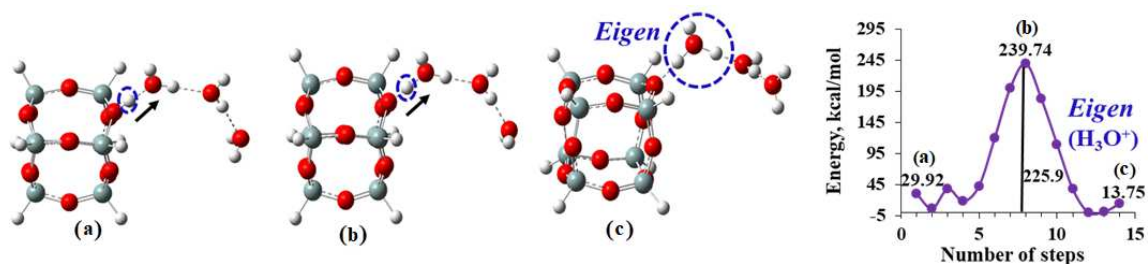


**Figure 5:** Reaction pathway and respective energy barrier (in kcal/mol) for the different conformation of the Eigen cation at POSS- $W_3$  interface (at PBE+D3/TZVP method). (a), (b) and (c) correspond to snapshots at the beginning, at the maximum of the energy barrier and at the end of the reaction, respectively. The blue dotted circle indicates the proton localized sites.

To get information about the conduction of proton, we performed nudged elastic band analyses for POSS- $H^+@W_{3a}$ , POSS- $H^+@W_{4a}$  and POSS- $H^+@W_{4c}$  clusters. Computations suggest that POSS- $H^+@W_{3a}$  and POSS- $H^+@W_{4a}$  isomers are more stable than the other clusters. Thus, we selected POSS- $H^+@W_{4c}$  model for cyclic pathway. The detailed reaction pathway with energy barrier analysis are shown in Figure 5 and Figure S6 for POSS- $H^+@W_3$ , POSS- $H^+@W_{4a}$  and POSS- $H^+@W_{4c}$  clusters. Our study reveals that the activation energy required for Eigen cation is  $\sim 240$  kcal/mol, whereas Zundel ion formation requires less energy (i.e.  $\sim 184$  kcal/mol). This documents the destabilization of Zundel ion at this interface favoring the formation of an Eigen core. This is also in line with the BE analysis and IR shifting values discussed in previous section.

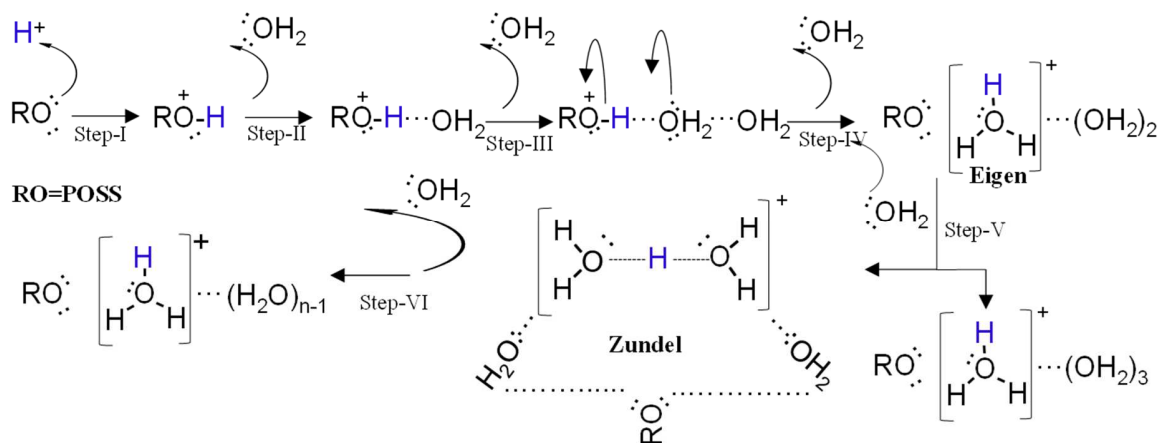


**Figure 6:** Proposed mechanism for the proton transfer from the POSS framework into water clusters. The excess proton in the POSS- $H^+@W_n$  clusters is shown in blue color.

The present work identifies a proton transfer pathway through water wire, which corresponds to the well-known Grotthuss mechanism as illustrated in Figure 6. This figure shows the important steps with formation of Eigen  $\rightarrow$  Zundel  $\rightarrow$  Eigen features during hydration process. The present geometrical analysis reveals that the formation of Eigen feature requires a minimum of three water molecules whereas Zundel feature requires a minimum of four water molecules in the POSS-H<sup>+</sup>@W<sub>n</sub> clusters. Similar observation also found for the experimental and theoretical studies on proton exchange membrane fuel cell (PEMFC) materials (i.e. Nafion),<sup>53</sup> a hydrated form of protonated carbonic acid (PCA),<sup>3</sup> carborane acid (CA)<sup>17</sup> and trifluoromethanesulfonic acid (TA)<sup>54</sup> with water clusters (W<sub>n</sub>, where  $n = 1-6$ ). Moreover, the formation of Zundel ion requires a symmetrical arrangement of water molecules, whereas asymmetric hydration patterns dislocate into Eigen ion. The changes in bond distances upon attaching water molecules to POSS-H<sup>+</sup> suggest that the excess proton can jump from one molecule to other through H-bonded water chain during the hydration. Since the proton localized in the center of the water chain, the charge dissociation / association mechanism of water molecule plays a vital role in the formation of hydronium ion and the same interacts with the neighbor. This clearly reveals that the primary shell interaction of water molecule strength reduces during the migration of a proton.

The energetics of the clusters allow determining the minimal energy pathway to conduct proton through water chain via the identification of the most stable isomers, important for the proton hopping mechanism. The origin of the proton hopping mechanism is the existence of Eigen and Zundel cationic defects. The excess proton localized in the middle with the formation of Zundel feature illustrates the origin of proton conduction via the Zundel to Eigen transformation. When slight distortion happens in the molecular arrangement, H-bonds can favor the formation of Eigen or other short-lived species from symmetrical Zundel core. The transformation of Zundel-Eigen-Zundel is favored by increasing the number of water molecules within these clusters. Close scrutiny of the geometries, IR spectra and AIM electron density analysis of POSS-H<sup>+</sup>@W<sub>n</sub> clusters reveals that Zundel-type feature is observed when an even number of water molecules are arranged in cyclic clusters in conjunction with the formation of the symmetric configuration. However, the unequal/odd amount of hydration patterns are more favorable for the transfer of proton from Zundel to Eigen. Then it forms a Zundel core again for even number of water in the hydration process. This is in line with earlier reports, which revealed that proton migration in linear type clusters is more favorable than in the branched and cyclic motifs.<sup>3,17,54</sup> This is because of the formation of cyclic H-bonded water chain, of a large number of H-bonds and of the perfect localization of the Eigen core in the middle of the framework. A similar mechanism was recently found by Lowe et al.<sup>22</sup> at the silica-water interface.

The BEs of the POSS-H<sup>+</sup>@W<sub>n</sub> clusters agree well with the earlier reports on proton transfer models such as PCA, CA and TA with water clusters (where  $n = 1-6$ ).<sup>3,17,54</sup> The BEs depend on the proton leaving

ability of the parent molecule. They will reflect the number of required water molecules to dissociate the proton from the acid. At the B3LYP/6-311++G\*\* level, the stabilization of the Eigen cation occurs at hexameric water clusters in linear model is computed  $\sim -119, -124, -196$  and  $-118$  (in kcal/mol) for POSS, PCA, CA and TA, respectively. For the branched types lower energies are derived: POSS ( $\sim -117$  kcal/mol), PCA ( $\sim -112$  kcal/mol) and TA ( $\sim -117$  kcal/mol). Note that the BEs of POSS-H<sup>+</sup>@W<sub>6</sub> clusters are in close agreement with the Nafion based triflic acid-water cluster model.<sup>54</sup> This confirms that the proton transfer ability of POSS moiety at solid-liquid interface is online with well-known PEMFCs such as Nafion. The main advantage of the POSS framework is that it is insoluble in water, chemicals and it presents a thermal stability even at elevated temperatures. The POSS moiety acts as H<sup>+</sup> source/carrier and at the same time water molecules act as transporter for the PEMFC materials.

## 5. Conclusion

This work presents the gas-phase geometries, binding energies, and infra-red spectral signatures of protonated POSS – water (POSS-H<sup>+</sup>@W<sub>*n*</sub>, where *n* = 1–6) clusters as calculated using DFT based B3LYP/6-311++G\*\* method. It is the first report on the prediction of Zundel features in POSS-H<sup>+</sup>@W<sub>*n*</sub> clusters interface and provide valuable information to detect the Zundel ion in such clusters. We reveal also the existence of Zundel → Eigen → Zundel features that are trapped at the POSS-water interface. Moreover, close scrutiny of linear chain isomers shows that the proton transfer occurs from one water molecule to another molecule *via* Grotthuss-type mechanism and these clusters are stabilized by the Eigen core with the W<sub>*n*</sub> clusters at the middle of the chain. It is interesting to note that the formation of the Eigen cation requires a minimum of three water molecules, whereas that of the Zundel ion needs four water molecules at the POSS-water interface. At the same time, both POSS moiety and water molecules act as an H<sup>+</sup> source and better transporter for the PEMFC materials, respectively. These features can enhance proton transport through the water chain at the microscopic hydration level. Such water molecules can be qualified as active water molecule, since it can accept a proton from POSS with simultaneous transfer of a proton to a neighboring water molecules. Since such mechanism was already found at the silica–water interface<sup>22</sup> and since the present work hints at its occurrence at nano-water clusters, it may be more general than usually thought, and we suggest that it should be investigated further, both by computational and experimental means, to improve our understanding of proton transport in water near interfaces.

## Acknowledgment

K. R. M. and S. K. thank SRM Institute of Science and Technology (SRM-IST) Research Fellowship for his research work. M. P. thanks the Department of Science and Technology-Science and Engineering Research Board (DST-SERB) of India for the financial support (Grant number:

ECR/2017/000891). The authors also thank SRM Supercomputer Centre (HPCC), SRM Institute of Science and Technology for providing the computational facility and financial support, and acknowledge access to HPC platforms provided by a GENCI grant (A0090807069).

### **Appendix A. Supplementary data**

Supporting Information: This file contains the AIM Analysis and the vibrational Analysis of POSS-H<sup>+</sup>@W<sub>n</sub> (where n=1 to 6) and the corresponding tables and figures. Reaction pathway and energy barrier analysis of POSS-H<sup>+</sup>@W<sub>4</sub> clusters using NEB method.

## REFERENCES

- <sup>1</sup> Schmitt, U. W.; Voth, G. A. Multistate empirical valence bond model for proton transport in water. *J. Phys. Chem. B* **1998**, *102*, 5547–5551.
- <sup>2</sup> Voth, G. A. Computer simulation of proton solvation and transport in aqueous and biomolecular systems. *Acc. Chem. Res.* 2006, *39*, 143–150.
- <sup>3</sup> Prakash, M.; Subramanian, V.; Gadre, S. R. Stepwise hydration of protonated carbonic acid: a theoretical study. *J. Phys. Chem. A* **2009**, *113*, 12260–12275.
- <sup>4</sup> Achtyl, J. L. et al. Aqueous proton transfer across single-layer graphene. *Nat. Commun.* **2015**, *6*, 6539.
- <sup>5</sup> K. Boussouf, T. Khairat, M. Prakash, N. Komih, G. Chambaud and M. Hochlaf Structure, spectroscopy and bonding within the  $Zn^{q+}$ -imidazole<sub>n</sub> (q = 0, 1, 2; n = 1 - 4) clusters and implications for ZIFs and Zn-enzymes. *J. Phys. Chem. A* **2015**, *119*, 11928–11940.
- <sup>6</sup> Weichselbaum, E.; Österbauer, M.; Knyazev, D. J.; Batishchev, O. V.; Akimov, S. A.; Nguyen, T. H.; Zhang, C.; Knör, G.; Agmon, N.; Carloni, P.; Pohl, P. Origin of proton affinity to membrane/water interfaces. *Scientific Reports* **2017**, *7*, 4553.
- <sup>7</sup> Wang, M.; Jaegers, N. R.; Lee, M. S.; Wan, C.; Hu, J. Z.; Shi, H.; Mei, D.; Burton, S. D.; Camaioni, D. M.; Gutiérrez, O. Y.; Glezakou, V. A.; Rousseau, R.; Wang, Y.; Genesis, J. A. L. Stability of hydronium ions in zeolite channels. *J. Am. Chem. Soc.*, **2019**, *141*, 3444–3455.
- <sup>8</sup> de Grotthuss, C. J. T. Sur la décomposition de l'eau et des corps qu'elle tient en dissolution à l'aide de l'électricité galvanique. *Ann. Chim.* **1806**, *58*, 54–73.
- <sup>9</sup> Kreuer, K. D.; Rabenau, A.; Weppner, W. Vehicle mechanism, a new model for the interpretation of the conductivity of fast proton conductors. *Angew. Chem. Int. Ed. Engl.* **1982**, *21*, 208–209.
- <sup>10</sup> Mauritz, K. A.; Moore, R. B. State of understanding of Nafion. *Chem. Rev.* **2004**, *104*, 4535–4585.
- <sup>11</sup> Li, G.; Wang, L.; Ni, H.; Pittman Jr, C. U. Polyhedral oligomeric silsesquioxane (POSS) polymers and copolymers: A Review. *J. Inorg. Organomet. Polym.* **2002**, *11*, 123–54.
- <sup>12</sup> Baney, R. H.; Itoh, M.; Sakakibara, A.; Suzuki, T. Silsesquioxanes. *Chem. Rev.* **1995**, *95*, 1409–1430.
- <sup>13</sup> Shea, K. J.; Loy, D. A. Bridged polysilsesquioxanes Molecular-engineered hybrid organic–inorganic materials. *Chem. Mater.* **2001**, *13*, 3306–3319.
- <sup>14</sup> Kuo, SW.; Chang, FC. POSS related polymer nanocomposites. *Prog. Polym. Sci.* **2011**, *36*, 1649–1696.
- <sup>15</sup> Cordes, D. B.; Lickiss, P. D.; Rataboul, F. Recent developments in the chemistry of cubic polyhedral oligosilsesquioxanes. *Chem. Rev.* **2010**, *110*, 2081–2173.
- <sup>16</sup> Cuma, M.; Schmitt, U. W.; Voth, G. A. A multi-state empirical valence bond model for weak acid dissociation in aqueous solution. *J. Phys. Chem. A* **2001**, *105*, 2814–2823.
- <sup>17</sup> Prakash, M.; Subramanian, V. Structure, stability and spectral signatures of monoprotic carborane acid–water clusters (CBW<sub>n</sub>, where n= 1–6). *Phys. Chem. Chem. Phys.* **2011**, *13*, 21479–21486
- <sup>18</sup> Quaranta, V.; Hellström, M.; Behler, J. Proton-transfer mechanisms at the water–ZnO interface: The role of presolvation. *J. Phys. Chem. Lett.* **2017**, *8*, 1476–1483.
- <sup>19</sup> Leung, K.; Criscenti, L. J.; Knight, A. W.; Ilgen, A. G.; Ho, T. A.; Greathouse, J. A. Concerted metal cation desorption and proton transfer on deprotonated silica surfaces. *J. Phys. Chem. Lett.* **2018**, *9*, 5379–5385.
- <sup>20</sup> Wang, S.; Wahiduzzaman, M.; Davis, L.; Tissot, A.; Shepard, W.; Marrot, J.; Martineau-Corcos, C.; Hamdane, D.; Maurin, G.; Devautour-Vinot, S. A robust zirconium amino acid metal-organic framework for proton conduction. *Nat. Commun.* **2018**, *9*, 4937.
- <sup>21</sup> Mileo, P. G. M.; Adil, K.; Davis, L.; Cadiou, A.; Belmabkhout, Y.; Aggarwal, H.; Maurin, G.; Eddaoudi, M.; Devautour-Vinot, S. Achieving superprotonic conduction with a 2D fluorinated metal–organic framework. *J. Am. Chem. Soc.* **2018**, *140*, 13156–13160.
- <sup>22</sup> Lowe, B. M.; Skylaris, C.-K.; Green, N. G. Acid-base dissociation mechanisms and energetics at the silica–water interface: An activationless process. *J. Colloid and Interface Sci.* **2015**, *451*, 231–244
- <sup>23</sup> Wang, C.; Clark, J. K.; Kumar, M.; Paddison, S. J. An ab initio study of the primary hydration and proton transfer of CF<sub>3</sub>SO<sub>3</sub>H and CF<sub>3</sub>O (CF<sub>2</sub>)<sub>2</sub> SO<sub>3</sub>H: Effects of the hybrid functional and inclusion of diffuse functions. *Solid State Ionics* **2011**, *199*, 6–13.
- <sup>24</sup> Losch, P.; Joshi, H. R.; Vozniuk, O.; Grünert, A.; Ochoa-Hernández, C.; Jabraoui, H.; Badawi, M.; Schmidt, W. Proton mobility, intrinsic acid strength, and acid site location in zeolites revealed by varying temperature infrared spectroscopy and density functional theory studies. *J. Am. Chem. Soc.*, **2018**, *140*, 17790–17799.
- <sup>25</sup> Xing, D.; Kerres, J. Improved performance of sulfonated polyarylene ethers for proton exchange membrane fuel cells. *Polym. Adv. Technol.* **2006**, *17*, 591–597.

- <sup>26</sup> Hartmann-Thompson, C.; Merrington, A.; Carver, P. I.; Keeley, D. L.; Rousseau, J. L.; Hucul, D.; Bruza, K. J.; Thomas, L. S.; Keinath, S. E.; Nowak, R. M.; Katona, D. M.; Santurri, P. R. Proton-conducting polyhedral oligosilsesquioxane nanoadditives for sulfonated polyphenylsulfone hydrogen fuel cell proton exchange membranes. *J. Appl. Polym. Sci.* **2008**, *110*, 958–974.
- <sup>27</sup> Becke, A. D. Density-functional exchange-energy approximation with correct asymptotic behavior. *Phys. Rev. A* **1988**, *38*, 3098.
- <sup>28</sup> Becke, A. D. Density-functional thermochemistry. III. The role of exact exchange. *J. Chem. Phys.* **1993**, *98*, 5648–5652.
- <sup>29</sup> Kuo, J. L.; Xie, Z. Z.; Bing, D.; Fujii, A.; Hamashima, T.; Suhara, K. I.; Mikami, N. Comprehensive analysis of the hydrogen bond network morphology and OH stretching vibrations in protonated methanol–water mixed clusters,  $H^+(MeOH)_1(H_2O)_n$  ( $n = 1-8$ ) *J. Phys. Chem. A*, **2008**, *112*, 10125–10133.
- <sup>30</sup> Jiang, J. C.; Chaudhuri, C.; Lee, Y. T.; Chang, H.-C. Hydrogen Bond Rearrangements and Interconversions of  $H^+(CH_3OH)_4H_2O$  Cluster Isomers. *J. Phys. Chem. A* **2002**, *106*, 10937–10944.
- <sup>31</sup> Wu, C. C.; Lin, C. K.; Chang, H. C.; Jiang, J. C.; Kuo, J. L.; Klein, M. L. Protonated clathrate cages enclosing neutral water molecules:  $H^+(H_2O)_{21}$  and  $H^+(H_2O)_{28}$ . *J. Chem. Phys.* **2005**, *122*, 074315.
- <sup>32</sup> Lin, C. K.; Wu, C. C.; Wang, Y. S.; Lee, Y. T.; Chang, H. C.; Kuo, J. L.; Klein, M. L. Vibrational predissociation spectra and hydrogen-bond topologies of  $H^+(H_2O)$ . *Phys. Chem. Chem. Phys.* **2005**, *7*, 938–944.
- <sup>33</sup> Frisch, M. J.; Trucks, G. W.; Schlegel, H. B.; Scuseria, G. E.; Robb, M. A.; Cheeseman, J. R.; Scalmani, G.; Barone, V.; Petersson, G. A.; Nakatsuji, H.; Li, X.; Caricato, M.; Marenich, A. V.; Bloino, J.; Janesko, B. G.; Gomperts, R.; Mennucci, B.; Hratchian, H. P.; Ortiz, J. V.; Izmaylov, A. F.; Sonnenberg, J. L.; Williams-Young, D.; Ding, F.; Lipparini, F.; Egidi, F.; Goings, J.; Peng, B.; Petrone, A.; Henderson, T.; Ranasinghe, D.; Zakrzewski, V. G.; Gao, J.; Rega, N.; Zheng, G.; Liang, W.; Hada, M.; Ehara, M.; Toyota, K.; Fukuda, R.; Hasegawa, J.; Ishida, M.; Nakajima, T.; Honda, Y.; Kitao, O.; Nakai, H.; Vreven, T.; Throssell, K.; Montgomery, J. A., Jr.; Peralta, J. E.; Ogliaro, F.; Bearpark, M. J.; Heyd, J. J.; Brothers, E. N.; Kudin, K. N.; Staroverov, V. N.; Keith, T. A.; Kobayashi, R.; Normand, J.; Raghavachari, K.; Rendell, A. P.; Burant, J. C.; Iyengar, S. S.; Tomasi, J.; Cossi, M.; Millam, J. M.; Klene, M.; Adamo, C.; Cammi, R.; Ochterski, J. W.; Martin, R. L.; Morokuma, K.; Farkas, O.; Foresman, J. B.; Fox, D. J. Gaussian 16, *Gaussian, Inc.*: Wallingford CT, **2016**.
- <sup>34</sup> Dennington, R.; Keith, T. A.; Millam, J. M. GaussView 6.0.16, Shawnee Mission; SemichemInc, **2016**.
- <sup>35</sup> Zhurko, G. A.; Zhurko, D. A. Chemcraft Program, academic version 1.8, **2015**.
- <sup>36</sup> Biegler-Konig, F.; Schonbohm, J.; Derdau, R.; Bayles, D.; Bader, R. F. W. *AIM 2000, version 1*; Bielefeld, Germany, **2000**.
- <sup>37</sup> Vandevondele, J.; Krack, M.; Mohamed, F.; Parrinello, M.; Chassaing, T.; Hutter, J. QUICKSTEP: Fast and Accurate Density Functional Calculations Using a Mixed Gaussian and Plane Waves Approach. *Comput Phys Commun.* **2005**, *167* (2), 103–128.
- <sup>38</sup> Perdew, J. P.; Burke, K.; Ernzerhof, M. Generalized Gradient Approximation Made Simple. *Phys. Rev. Lett.* **1996**, *77* (3), 3865–3868.
- <sup>39</sup> Grimme, S. Semiempirical Hybrid Density Functional with Perturbative Second-Order Correlation Semiempirical Hybrid Density Functional with Perturbative Second-Order Correlation. *J. Chem. Phys.* **2006**, *124*, 034108–034116.
- <sup>40</sup> Grimme, S.; Antony, J.; Ehrlich, S.; Krieg, H. A Consistent and Accurate Ab Initio Parametrization of Density Functional Dispersion Correction (DFT-D) for the 94 Elements H-Pu. *J. Chem. Phys.* **2010**, *132*, 154104–15123.
- <sup>41</sup> Mouhat, F.; Coudert, F.-X.; Bocquet, M. L. Structure and chemistry of graphene oxide in liquid water from first principles. *Nat Commun.*, **2020**, *11*, 1566.
- <sup>42</sup> Motta, A.; Gageot, M.-P.; Costa, D. Ab Initio Molecular Dynamics Study of the AlOOH Boehmite/Water Interface: Role of Steps in Interfacial Grotthus Proton Transfers. *J. Phys. Chem. C*, **2012**, *116*, 12514–12524.
- <sup>43</sup> Nguouana-Wakou, B. F.; Cornette, P.; Corral Valero, M.; Costa, D.; Raybaud, P. An Atomistic Description of the  $\gamma$ -Alumina/Water Interface Revealed by Ab Initio Molecular Dynamics. *J. Phys. Chem. C*, **2017**, *121*, 10351–10363.
- <sup>44</sup> Grosjean, B.; Robert, A.; Vuilleumier, R.; Bocquet, M.-L. Spontaneous liquid water dissociation on hybridised boron nitride and graphene atomic layers from ab initio molecular dynamics simulations. *Phys. Chem. Chem. Phys.*, **2020**, *22*, 10710–10716.
- <sup>45</sup> Applications of Polyhedral Oligomeric Silsesquioxanes edited by Claire Hartmann-Thompson Springer Dordrecht Heidelberg; London New York., **2011**.
- <sup>46</sup> Park, M.; Shin, I.; Singh, N. J.; Kim, K. S. Eigen and Zundel forms of small protonated water clusters: Structures and infrared spectra. *J. Phys. Chem. A*, **2007**, *111*, 10692–10702.
- <sup>47</sup> Boys, S. F.; Bernardi, F. D. The calculation of small molecular interactions by the differences of separate total energies. Some procedures with reduced errors. *Mol. Phys.* **1970**, *19*, 553–566.

- 
- <sup>48</sup> Grimme, S.; Antony, J.; Ehrlich, S.; Krieg, H. A consistent and accurate ab initio parametrization of density functional dispersion correction (DFT-D) for the 94 elements H-Pu. *J. Chem. Phys.*, **2010**, *132*, 154104.
- <sup>49</sup> Parthasarathi, R.; Subramanian, V.; Sathyamurthy, N. Hydrogen bonding in protonated water clusters: An atoms in molecules perspective. *J. Phys. Chem. A*, **2007**, *111*, 13287–13290.
- <sup>50</sup> Nibu, Y.; Marui, R.; Shimada, H. IR spectroscopy of 2-fluoropyridine–water clusters in the electronic excited states. *Chem. Phys. Lett.* **2007**, *442*, 7–11.
- <sup>51</sup> Corradini, D.; Coudert, F.-X.; Vuilleumier, R. Carbon dioxide transport in molten calcium carbonate occurs through an oxo-Grotthuss mechanism via a pyrocarbonate anion. *Nat. Chem.* **2016**, *8*, 454-460.
- <sup>52</sup> Haigis, V.; Coudert, F.-X.; Vuilleumier, R.; Boutin, A. Investigation of structure and dynamics of the hydrated metal–organic framework MIL-53(Cr) using first-principles molecular dynamics. *Phys. Chem. Chem. Phys.* **2013**, *15*, 19049-19056.
- <sup>53</sup> Li, T.; Wlaschin, A.; Balbuena, P. B. theoretical studies of proton transfer in water and model polymer electrolyte systems. *Ind. Eng. Chem. Res.*, **2001**, *40*, 4789–4800.
- <sup>54</sup> Prakash, M.; Subramanian, V. Ab initio and density functional theory (DFT) studies on triflic acid with water and protonated water clusters. *J. Mol. Model.* **2016**, *22*, 293.